Probing Interstellar and Circumstellar Material on the Line of Sight to Protoplanetary Disks

Matthew McJunkin, Kevin France

University of Colorado at Boulder

Abstract

Absorption line spectroscopy provides the most straightforward means of determining the composition and physical state of material along the line of sight towards protostars. Using observations of 31 gas-rich classical T Tauri stars (CTTSs) and Herbig Ae/Be stars obtained with the *Hubble Space Telescope* (*HST*), we present new measurements of the molecular disk properties and the interstellar dust attenuation towards these objects. The high-sensitivity of the *HST*-Cosmic Origins Spectrograph has enabled the first ultraviolet detections of carbon monoxide (CO) absorption through protoplanetary disks. We compare the data from six objects with strong CO absorption to spectral synthesis models to determine the column density and temperature of the CO gas. We find column densities in the range log(N(CO)) = 16 – 18 and temperatures of 300 – 700 K, assuming thermal equilibrium.

Reddening due to interstellar grains is notoriously challenging to determine towards CTTSs owing to veiling of the photospheric emission by excess flux due to accretion shocks. We present a new approach to this problem by using accurate interstellar atomic hydrogen column densities to determine the selective reddening using the well-known relationship between these quantities. We present new values of the optical extinction (A_V) for the 31 CTTSs and Herbig stars. Our general result is that literature values for A_V typically overestimate the reddening on CTTS sightlines.

Targets and Observations

31 young (~ 0.6 - 20 Myr) Herbig Ae/Be and CTTS Lyman-α (Lyα) emission profiles taken with the Cosmic Origins Spectrograph and Space Telescope Imaging Spectrograph on *HST* are modeled to determine interstellar neutral hydrogen (HI) column densities. The majority of the targets are located in the Taurus-Auriga, Chamaeleon I, and η Chamaeleontis star-forming regions. The rest belong to other associations and isolated systems. Six of the CTTSs far-UV spectra are also fit with a CO absorption model to determine CO column densities and temperatures. Targets studied with the CO model have moderate-to-high inclination (35° - 77°) and six clean vibrational bands detected.

Figure 1 - *(Below)* Components of the normalized Lyα model. The broad emission line is the green line, the narrow emission is the red line and the unabsorbed model Lyman-α emission is the blue line. The HI transmission curve is plotted in black.

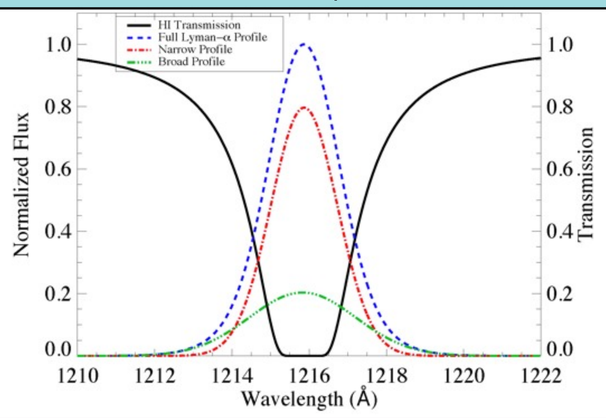

Observed CO Absorption Lines

Figure 2 - The 9 far-UV CO rotational absorption bands marked in the targets. The bands are (v' - 0) with v' = 8 on the left over to v' = 0 on the right. The (0 - 0) and (5 - 0) bands are often contaminated, and (8 - 0) has low signal-to-noise. They are not fit.

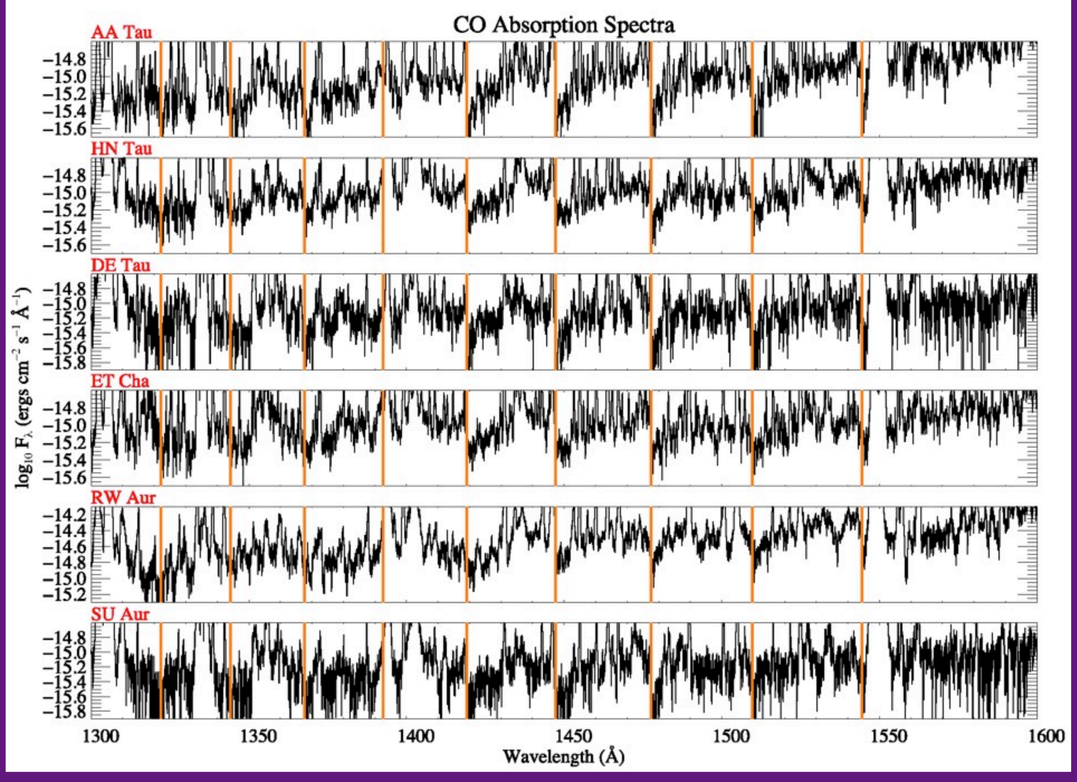

Model Fits

We search a grid of parameter space for the best-fit values using a least squares minimization. Fitting the HI absorption against the stellar Lyα profile yields a measurement of the reddening that is not confused by veiling. We only fit the red side of the Lyα profile to reduce contamination from outflow absorbers. The Lyα model is composed of a broad and narrow gaussian emission profile and a Voigt HI absorption profile (shown in Figure 1). The broad and narrow emission are characterized by a heliocentric velocity, full-width half-max, and amplitude while the absorption profile is characterized by a heliocentric velocity, Doppler *b*-value, and column density. The HI best-fit column density range is log(N(HI)) = 19.58 - 21.05 for all 31 targets.

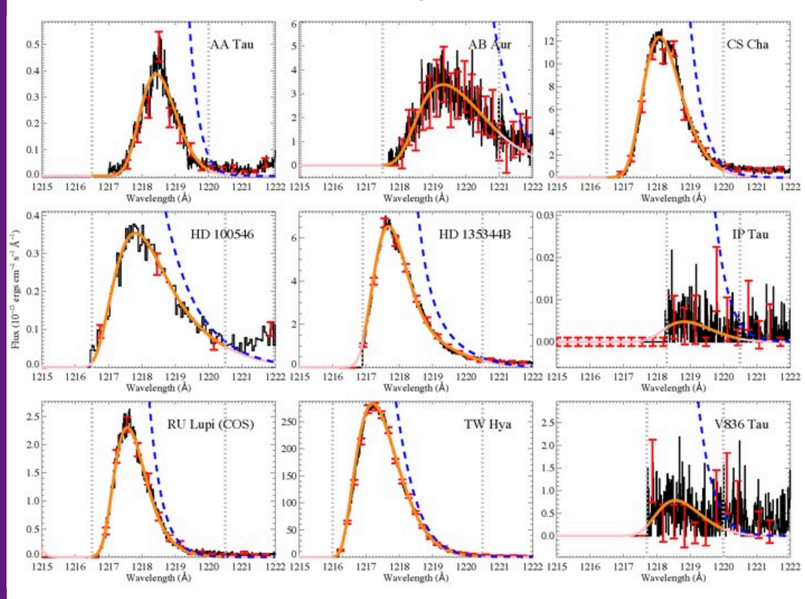

Figure 3 - *(Left)* Selected Lyα model fits. The data is in black, and the fit is in orange. The wavelength region that is fit is marked by vertical dashed lines. Some targets have less reliable fits due to no Lyα flux detected or noise (IP Tau and V836 Tau here) which are pink points in Figure 5.

Our CO model takes values for the ^{12}CO and ^{13}CO column densities, the rotational temperature of the CO, the Doppler *b*-value, and the radial velocity shift of the CO. We use the detected and uncontaminated (1 - 0), (2 - 0), (3 - 0), (4 - 0), (6 - 0), and (7 - 0) ro-vibrational bands (seen in Figure 2) to simultaneously constrain the best-fit values. The fit parameters range from b = 0.5 - 1.4 km s^{-1}, log(N(^{12}CO)) = 16.0 - 17.8, log(N(^{13}CO)) = 14.7 - 16.7, $T_{rot}(CO)$ = 300 - 700 K, and v_{CO} = 1.4 - 28.0 km s^{-1}.

Figure 4 - *(Below)* Low-v' model fits for two of the targets fit with the CO absorption model. The best-fit model parameters are listed in Table 1 to the right for all six targets included in the CO model fits. The data have been continuum normalized and the ^{13}CO bandhead has been marked to clearly show the two different CO species. The data is in black and the model is in orange.

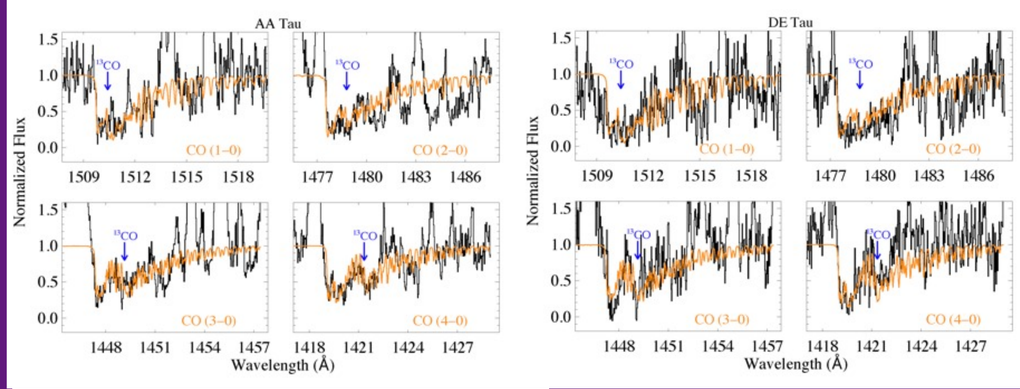

Results

We convert our HI column density measurements to visual extinction using the Bohlin et al. (1978) relation. Our A_V measurements are generally lower than those seen in the literature. Many A_V values listed in the literature require log(N(HI)) columns of 21 or more, which would extinguish the Lyα profile completely, which we do not observe.

Figure 5 - *(Below)* Literature A_V values compared to our computed HI column densities. Black points are targets with reliable fits, while pink points are targets with less reliable fits. The Bohlin et al. (1978) relation between HI column density and A_V for three R_V values is plotted with points corresponding to our calculated A_V values.

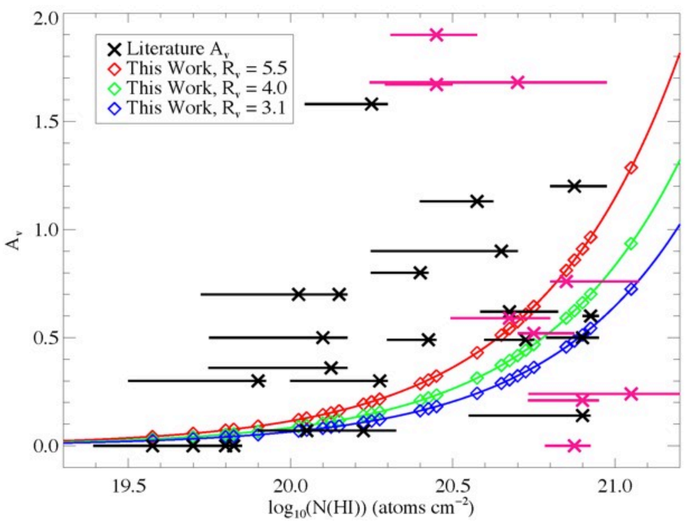

We also compare our A_V values to X-ray, optical, and IR extinction measurements and again find that our values are typically smaller.

Figure 6 - *(Below)* Comparison of our calculated A_V values with optical, IR, and other literature extinction values. Dashed lines show a 1:1 relation.

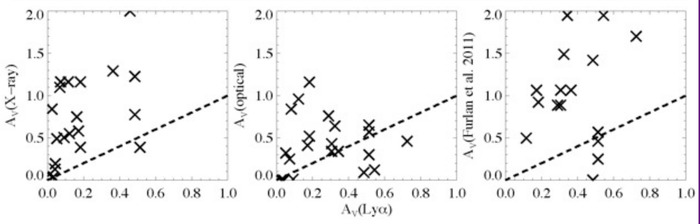

Our circumstellar CO rotational temperatures agree well with UV CO fluorescence rotational temperatures, but are cooler than inner disk CO temperatures from IR CO emission studies. The CO velocities rule out an origin in a fast-moving disk wind, and our derived temperatures and densities are consistent with models for disk heights of $z/r \sim 0.6$. This CO location constrains the inclination of the disks to be $\gtrsim 60°$ in order to intercept the absorbing gas in the model. Better inclination measurements for stars that show CO absorption, but have lower measured extinctions (DE Tau) are needed.

Table 1 - *(Below)* The best-fit parameters for the six targets fit with the CO absorption model.

Target	log(N(^{12}CO))	log(N(^{13}CO))	*b* (km/s)	$T_{rot}(CO)$ (K)	v_{CO} (km/s)
AA Tau	16.9	15.5	1.4	450	24.7
DE Tau	17.2	16.0	1.4	450	1.4
HN Tau	16.0	15.2	1.4	700	28.0
RECX-15	17.8	16.7	0.5	350	18.2
RW Aur	16.9	14.7	0.6	300	20.0
SU Aur	17.4	15.5	1.2	350	16.3

Matthew (right) would like to thank Greg Herczeg, Eric Schindhelm, Christian Schneider, Lynne Hillenbrand, and Suzan Edwards for their helpful comments.

For more information:

matthew.mcjunkin@colorado.edu